

# COMPLEX IMPEDENCE SPECTRAL AND AMAGNETIC STUDIES OF SILVER DOPED STRONTIUM HEXAFERRITE MAGNETIC NANOPARTICLES

K. Alamelu Mangai

.Department of Physics, Vel Tech High Tech Dr. Rangarajan Dr. Sakunthala Engineering College,  
Avadi, Chennai

## ABSTRACT

Silver doped  $\text{SrFe}_{12}\text{O}_{19}$  samples synthesized by solgel method based on decomposition of metal nitrates were subjected to impedance and magnetic studies. Results show that Ag doping decreases the magnetization and coercivity of nanoparticles. By increasing the Ag content in the samples the saturation magnetization shows interesting temperature dependent behavior. It was realized that magnetization of smaller particles show higher sensitivity to temperature variations than larger particles. From the impedance study the Nyquist plot confirms the existence of non-Debye type relaxation in the materials. Curie temperature ( $T_c$ ) and polaron activation energy in ferromagnetic and paramagnetic regions were estimated by using resistivity curves.

## 1. INTRODUCTION

Hexagonal M-type  $\text{S}$  plays an important role in hard magnetic materials due to their numerical application in microwave applications, high energy recording media, magneto optic media, magnetic components etc. As compared to widely used AlNiCo magnets, sintered strontium ferrites have several distinct properties such as relatively large saturation magnetisation, superior coercivity, high uniaxial magnetic crystalline anisotropy, chemical stability and corrosion resistance which made this material suitable for many applications.

Magnetic nanoparticle systems exhibiting superparamagnetic behavior shows no remanence and coercivity for keeping high saturation magnetization and have potential applications in biomedicine [1-2], magnetic drug delivery, cell sorting systems [3-4] and in magnetic refrigeration technology [5-6]. These applications require biocompatible magnetic nanomaterials. The silver doped ferrites meet these requirements but are not yet synthesized in the nano form. However the formation of bulk silver ferrite was reported by Croft et al [7].

The addition of silver to strontium hexaferrite will provide a new composite material with good

magnetic behavior. The influence of magnetic and antibacterial properties can make this material unique for applications in biomedicine. In this chapter we report the synthesis, characterization and magnetic studies of nano silver ferrite composite.

In the present work the effect of Ag substitution on magnetic and dielectric  $\text{SrAg}_x\text{Fe}_{(12-x)}\text{O}_{19}$ , ( $x=0.1, 0.2, 0.3$ ) nanoparticles has been reported. Vibrating sample magnetometer and Dielectric measurements.

## 2. EXPERIMENTAL PROCEDURE

### Synthesis of strontium hexaferrites

Silver substituted strontium hexagonal ferrite nano composites  $\text{SrAg}_x\text{Fe}_{(12-x)}\text{O}_{19}$  with  $0.1 \leq x \leq 0.3$  in steps of 0.1 by our earlier work [8]. For details of synthesis process the readers may refer our article in this journal. The samples were well polished and coated by silver paste for impedance measurements.

### 3. Methods and Characterization

Electrical conductivity of the investigated samples was measured in a wide range of temperature from the temperature 273K up to 573K in static air using

Novo control broadband dielectric spectrometer in the frequency range of 1Hz – 40 MHz over a temperature of 0K – 573K. The ac conductivity, the dielectric constant and the loss tangent  $\tan \delta$  as functions of frequency at different temperatures have been studied in detail and reported elsewhere.

#### 4. RESULTS AND DISCUSSION

##### 4.1. Complex impedance Analysis

From the dielectric study the real and imaginary parts of the dielectric constant have been obtained and the complex impedance spectra have been plotted for various temperatures. Figure.9 (a-c) Shows the complex impedance spectra (Nyquist Plot) of  $\text{SrAg}_{(1-x)}\text{Fe}_{(12-x)}\text{O}_{19}$  compounds at different temperatures. Appearance of single semi-circle shows that electrical properties in the materials are mainly due to the contribution of bulk effects. The formation of full, partial or no semi-circles mainly depends on the strength of relaxation and also experimentally available frequency range [9]. In Nyquist plots, the intercepts of semicircular arcs on real  $Z'$  axis gives the value of bulk resistance ( $R_b$ ) and is found to decrease with increase in temperature. It suggests the NTCR behavior of the compounds. The depressed semicircles whose centers lying below the real axis confirm the presence of non-Debye type relaxation in the materials [10].  $R_b$  is found to increase with increase in Ag content in the materials.

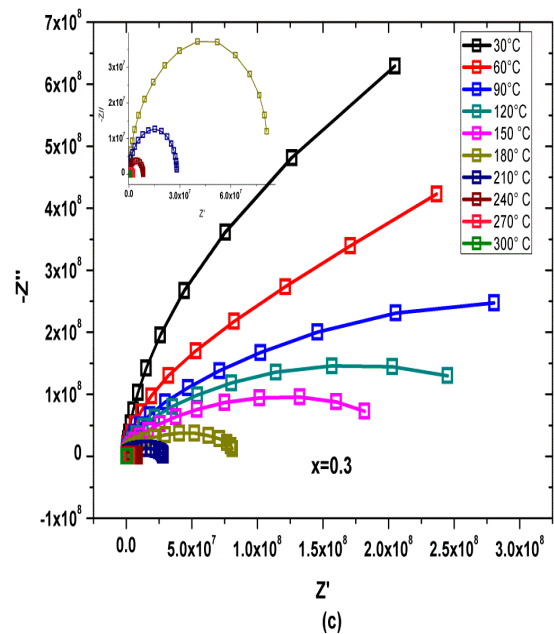
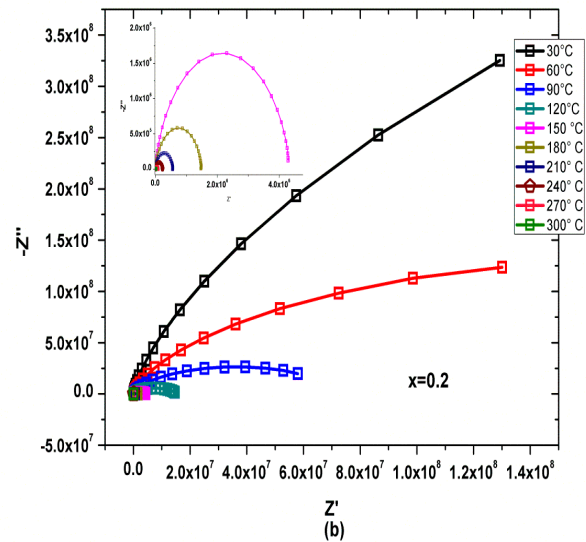
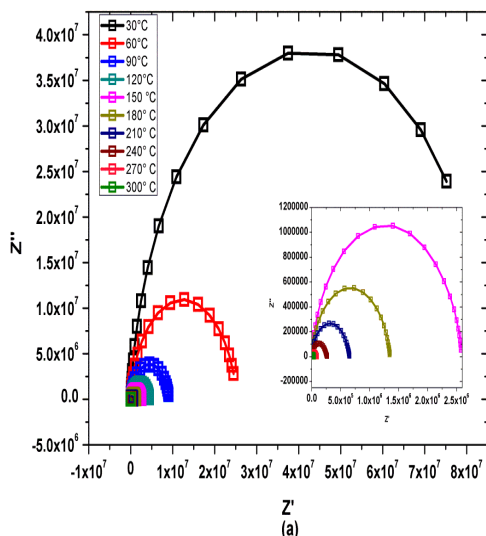


**Figure.9 Nyquist plot of  $\text{SrFe}_{12-x}\text{Ag}_x\text{O}_{19}$  ( $x=0.1, 0.2$  and  $0.3$ ) at different temperatures**

##### 4.2. Magnetic Characteristics

###### 4.2.1. Room Temperature Magnetization Measurement

Figure.10 (a-c) shows the room temperature magnetic hysteresis loops of  $\text{SrFe}_{12-x}\text{Ag}_x\text{O}_{19}$  ( $x=0.1, 0.2$  and  $0.3$ ). When an external field is applied, the domains already aligned, grow in the direction of applied field at the expense of their neighbours. The coercivity ( $H_c$ ), retentivity ( $M_r$ ), and saturation magnetization ( $M_s$ ) obtained from the hysteresis loops for the samples

are given in Table 1. Ag<sup>1+</sup> ion substitution on SrFe<sub>12</sub>O<sub>19</sub> leads to the decrease in both remanent and saturation magnetization. The decrease in magnetization is related to the magnetic moment of the constituent ions. This is due to the replacement of Fe<sup>3+</sup> ions by non-magnetic Ag<sup>1+</sup> ions and is responsible for the reduction in saturation magnetization and hence the remanence. As expected the saturation magnetization of the samples decreases by increasing the Ag<sup>1+</sup> content which may be due to the weakening of super exchange interaction of Fe<sup>3+</sup>-O-Fe<sup>3+</sup> and the structural distortion. The magnetic parameters derived from the hysteresis loops for all the samples were tabulated in Table 6.2. The magneton number is obtained using the relation [11].

$$\eta_B = \text{molecular weight} \times M_s / 5585$$

The values of magneton number decreases with increase in silver content indicating the paramagnetic behavior of ferrites. This is the cause of non-magnetic Ag<sup>3+</sup> substitution ions for Fe<sup>3+</sup> ions in the strontium hexaferrite with Also it is confirmed from the hysteresis loop that the high coercivity is attributed to the increase in anisotropy field H<sub>a</sub>. Hence it is clear that the hard magnetic behavior of the material is observed in silver substituted SrFe<sub>12</sub>O<sub>19</sub> nano composites. These properties make them desirable for applications in permanent magnets.

**Table.1. Effect of Ag<sup>3+</sup> substitution on the magnetic parameters of Ag<sub>x</sub>Fe<sub>12-x</sub>O<sub>19</sub> ferrites having x=0.1 – 0.3**

| SAM PLE | H <sub>c</sub> (G) | M <sub>s</sub> (emu/g) | M <sub>r</sub> (emu/g) | η <sub>B</sub> | M <sub>r</sub> /M <sub>s</sub> | K=H <sub>c</sub> μ <sub>0</sub> M <sub>s</sub> /2 |
|---------|--------------------|------------------------|------------------------|----------------|--------------------------------|---|
| A1      | 312<br>4.5         | 32.5<br>5              | 18.5<br>4              | 6.<br>19       | 0.5<br>7                       | 0.064   |
| A2      | 301<br>5.3         | 10.2<br>0              | 5.67                   | 1.<br>94       | 0.5<br>6                       | 0.0193  |
| A3      | 313<br>7           | 2.54                   | 1.45                   | 0.<br>48       | 0.5<br>7                       | 0.0050  |

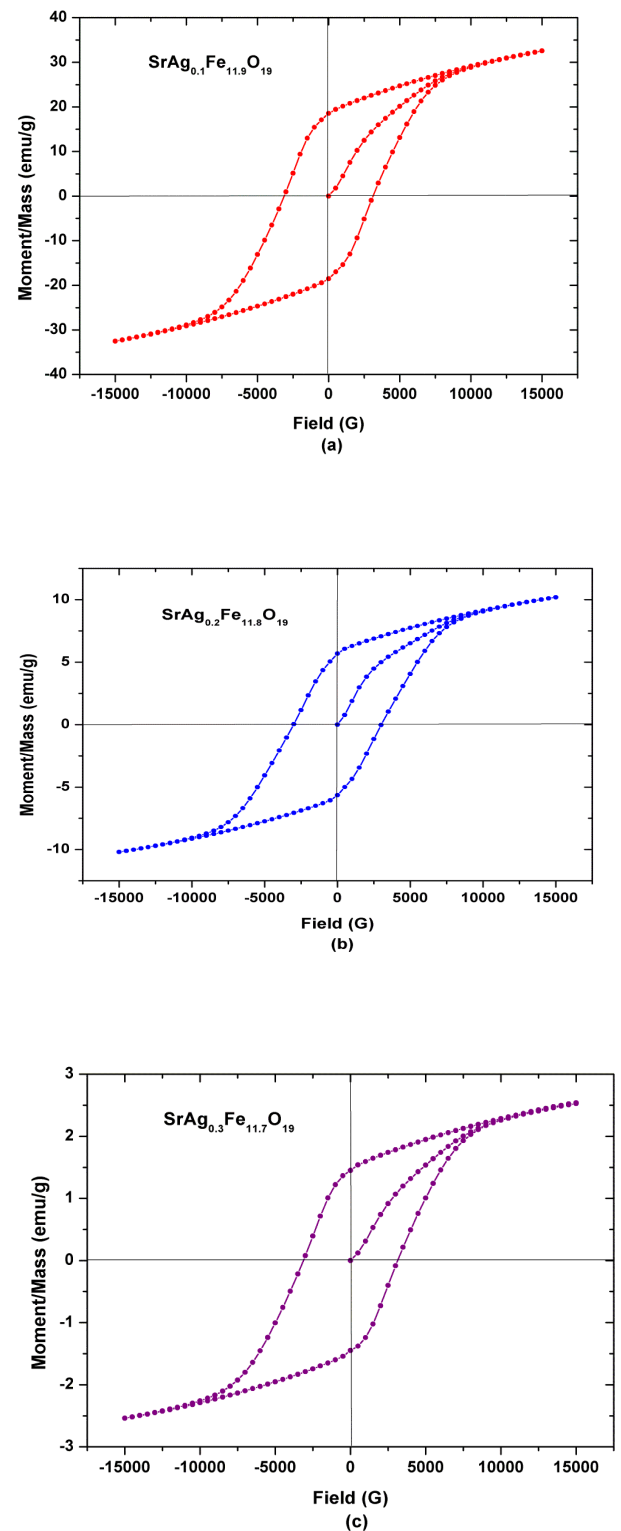


**Figure 10 Hysteresis curves of SrFe<sub>12-x</sub>Ag<sub>x</sub>O<sub>19</sub> (x=0.1, 0.2 and 0.3) at 800 °C using VSM**

#### 4.2.2. Temperature dependence of Magnetization measurements

The temperature dependent magnetization study was performed under a constant field of 100 Oe in order to determine the Curie transition, for  $\text{SrAg}_{0.3}\text{Fe}_{12-x}\text{O}_{19}$  is shown in Figure 11. The shape of the curve illustrates the characteristic peculiarity of Hopkinson effect [12-13]. As the crystallite size reduces below a certain value, the magnetic anisotropy decreases due to thermal effects and hence the magnetization becomes non-uniform. Therefore the resultant super paramagnetic relaxation shows a sharp peak at  $\sim 720$  K which is very close to the transition temperature  $\sim 730$  K. The sharp peak at this temperature is due to the transition from ferromagnetic state to super paramagnetic state. As the temperature is increased, the magnetization value is decreased gradually and a sudden increase in magnetization is observed. Above the blocking temperature  $T_B$ , the super paramagnetic relaxation takes place.

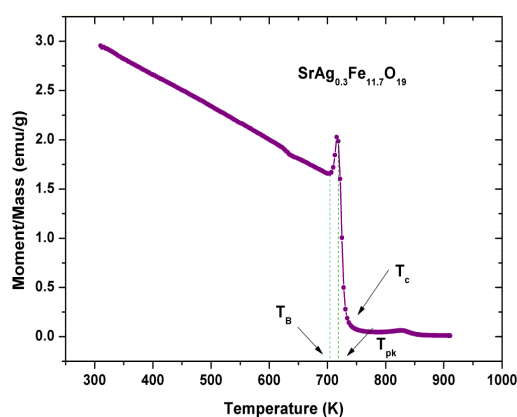


Figure 11 M-T curve of  $\text{SrFe}_{11.7}\text{Co}_{0.3}\text{O}_{19}$  at  $800^\circ\text{C}$  using VSM

#### 5. CONCLUSION

The hexagonal single phase materials of  $\text{SrFe}_{12-x}\text{Ag}_x\text{O}_{19}$  ( $x=0.1, 0.2$  and  $0.3$ ) system prepared by sol-gel route have subjected to Impedance and magnetic studies. The Nyquist plot drawn in impedance study confirms the presence of non-Debye type relaxation in the materials. Room temperature magnetic study reveals the ferromagnetic loop behavior for silver doped  $\text{SrFe}_{12}\text{O}_{19}$ . The reduction in saturation magnetization is due to the replacement of the non-magnetic  $\text{Ag}^{1+}$  ion. The temperature dependence of

magnetization observed in M-T curve explains the behavior of Hopkinson effect.

#### References

1. Gunther, L., 1988. Quantum theory of nucleation in ferromagnets. , 37(16), pp.9455–9459.
2. Krishna Surendra, M. et al., 2014. Magnetic hyperthermia studies on water-soluble polyacrylic acid-coated cobalt ferrite nanoparticles. *Journal of Nanoparticle Research*, 16(12).
3. Search, H. et al., 2005. Synthesis and characterization of functionalized silica-coated  $\text{Fe}_3\text{O}_4$  superparamagnetic nanocrystals for. , 1342.
4. Murthy, Y.L.N., Viswanath, I.V.K. & Rao, T.K., 2009. Synthesis and characterization of Nickel Copper Ferrite. , 1(4), pp.1308–1311.
5. Pope, N.M. et al., 1994. magnetic alginate beads as a solid support for positive selection of CD34+ cells. , 28, pp.449–457.
6. Rashad, M.M. & Ibrahim, I. a., 2011. Improvement of the magnetic properties of barium hexaferrite nanopowders using modified co-precipitation method. *Journal of Magnetism and Magnetic Materials*, 323(16), pp.2158–2164.
7. Shahriari, D.Y. et al., 2003. Direct synthesis of  $\text{AgInO}_2$ . , 64, pp.1437–1441.
8. (i) Alamelumangai et al Solgel Synthesis Of Silver Doped Strontium Hexaferrite Nanoparticles, *IntJ. Trendy research in Engg. and technology*. 2017, 1, pp.15-23 (ii) Ph.D thesis of Alamelumangai –Anna University, Chennai 2017
9. Ranjan, R. et al., 2014. Investigations of impedance and electric ceramics. , 5(3), pp.138–142.
10. Sathishkumar, G., Venkataraju, C. & Sivakumar, K., 2010. Synthesis , Structural and Dielectric Studies of Nickel Substituted Cobalt-Zinc Ferrite. , 2010(April), pp.19–24.
11. Gunther, L., 1988. Quantum theory of nucleation in ferromagnets. , 37(16), pp.9455–9459.
12. Irfan, S. et al., 2014. Synthesis of  $\text{Mn}_{1-x}\text{Zn}_x\text{Fe}_2\text{O}_4$  ferrite powder by co-precipitation method. *IOP Conference Series: Materials Science and Engineering*, 60, p.12048.
13. Ahmed, M.A., Helmy, N. & El-Dek, S.I., 2013. Innovative methodology for the synthesis of Ba-M hexaferrite  $\text{BaFe}_{12}\text{O}_{19}$  nanoparticles. *Materials Research Bulletin*, 48(9), pp.3394–3398.